Virology 528 (2019) 164–175

Contents lists available at ScienceDirect

Virology

journal homepage: www.elsevier.com/locate/virology

SERRATE, a miRNA biogenesis factor, affects viroid infection in *Nicotiana benthamiana* and *Nicotiana tabacum*

Nikoleta Kryovrysanaki[a,b], Anastasios Alexiadis[a,b], Alexandra M. Grigoriadou[b], Konstantina Katsarou[a], Kriton Kalantidis[a,b,*]

[a] Institute of Molecular Biology and Biotechnology, Foundation for Research and Technology, GR-7110 Heraklion, Crete, Greece
[b] Department of Biology, University of Crete, Vassilika Vouton, GR-71409 Heraklion, Crete, Greece

ARTICLE INFO

Keywords:
PSTVd
DCL1
microRNAs
RNA silencing
Viroid pathogenicity

ABSTRACT

Viroids are plant infecting, non - coding RNA molecules of economic importance. *Potato spindle tuber viroid* (PSTVd), the type species of *Pospiviroidae* family, has been shown to be affected by specific RNA silencing pathways. Dicer like 1 (DCL1), a key player in micro RNA (miRNA) pathway has been previously linked with PSTVd infectivity. In this report we aim to further dissect the interaction between the miRNA pathway and Pospiviroid virulence. We mainly focused on the Zinc-finger protein SERRATE (SE) a co-factor of DCL1 and core component of miRNA pathway. We generated *Nicotiana tabacum* and *Nicotiana benthamiana* SE knock-down plants exhibiting considerable miRNA reduction and strong phenotypic abnormalities. PSTVd infection of SE suppressed plants resulted in a significant viroid reduction, especially at the initial infection stages. This positive correlation between SE levels and viroid infectivity underlines its role in PSTVd life cycle and reveals the importance of the miRNA pathway upon viroid infection.

1. Introduction

Viroids are a class of infectious, single-stranded RNA (ssRNA) molecules of 250–401 nucleotides (nt) in length that often cause significant loses to plants of major economic importance (reviewed by Flores et al., 2011; Katsarou et al., 2015; Palukaitis, 2014; Rao and Kalantidis, 2015; Tsagris et al., 2008). According to their structural and functional characteristics, viroids are classified in two families: i) *Avsunviroidae* and ii) *Pospiviroidae* (Ahmed et al., 2014; Di Serio et al., 2014; Katsarou et al., 2015; Rao and Kalantidis, 2015). *Potato spindle tuber viroid* (PSTVd) is the type species of pospiviroids, and refers to a circular, single stranded RNA of 356–361 nt depending on the isolate (Owens, 2007; Tsagris et al., 2008).

Viroids do not encode for proteins, therefore their infectivity is tightly coupled to the transcriptional and processing machinery supplied by the host (Daros and Flores, 2004). RNA silencing, an ancient eukaryotic process referring to small RNA-mediated pathways, is known to play a key role in modulating host - pathogen interactions (Baulcombe, 2004; Ruiz-Ferrer and Voinnet, 2009). Main component of these pathways are the RNase III family endonucleases called Dicer-like (DCL) that produce double stranded short interfering RNAs (siRNAs) and micro RNAs (miRNAs) of 21–24 nt (Bologna and Voinnet, 2014). Four DCL proteins (DCL1, DCL2, DCL3 and DCL4) have been characterized in plants producing small RNAs (sRNAs) of 21, 22, and 24 nt 21nt that are implicated in different RNA silencing pathways (Bouché et al., 2006; Matzke et al., 2009; Schauer et al., 2002).

The role of RNA silencing as a host defense mechanism against foreign nucleic acid, including viruses and transposable elements in plants, is well studied (reviewed in Baulcombe, 2004; Pumplin and Voinnet, 2013). Several works have also attempted to elucidate the effect of RNA silencing on viroid infection (Daròs et al., 2006; Denti et al., 2004; Itaya et al., 2007, 2001; Landry and Perreault, 2005, 2004; Machida et al., 2007; Markarian et al., 2004; Martín et al., 2007; Martínez de Alba et al., 2002; Papaefthimiou et al., 2001; Wang et al., 2004). Owing to the structural and functional similarity between pre-miRNAs and viroids, it was proposed that viroid RNAs may function as miRNA - like precursors whose processing would lead to the generation of miRNA – like viroid derived small RNAs (vd-sRNAs) that could target host genes (Gomez et al., 2008; Markarian et al., 2004; Matoušek et al., 2007; Papaefthimiou et al., 2001; Wang et al., 2004). Other non-coding, pathogenic, virus-derived RNAs, known as satellite RNAs (satRNA), have been identified as inducers and targets of Post-transcriptional gene silencing (PTGS) and were shown to act like miRNAs to suppress host genes (Masuta and Takanami, 1989; Shimura et al., 2011; Smith et al.,

* Corresponding author.
E-mail addresses: nkrio@imbb.forth.gr (N. Kryovrysanaki), kriton@imbb.forth.gr (K. Kalantidis).

https://doi.org/10.1016/j.virol.2018.12.011
Received 19 September 2018; Received in revised form 14 December 2018; Accepted 15 December 2018
Available online 29 December 2018

2011; Wang et al., 2004). Similarly, in the *Avsunoviroidae* family there is evidence supporting a miRNA like role of vd-sRNAs: *Prunus persica* plants infected with *Peach latent mosaic viroid* (PLMVd) demonstrated the characteristic albinism phenotype which was attributed to RNA silencing - directed disease with the potential involvement of a vd-siRNA (Navarro et al., 2012a). However, it is still unclear whether this may be the case for viroids of the *Pospiviroidae* family. The identification of vd-siRNAs from the pathogenicity domain of PSTVd supported the idea of possible involvement of vd-sRNAs in symptom development (Diermann et al., 2010). In addition, tomato plants expressing hairpin RNA derived from the severe PSTVd^{RG1}strain, provided evidence that the hairpin-derived siRNAs directed RNA silencing of host genes leading to symptom development (Wang et al., 2004) although, this finding was not supported by later experiments (Schwind et al., 2009).

DCL1 and SERRATE (SE) are key factors of the miRNA pathway (reviewed in Xie et al., 2015). In cooperation with its binding partners HYPONASTIC LEAVES 1 (HYL1) (Dong et al., 2008; Kurihara and Watanabe, 2004) and SE (Dong et al., 2008; Iwata et al., 2013), DCL1 produces 21nt miRNAs from endogenous sequences carrying internal stem-loops (Schauer et al., 2002). DCL1 also facilitates the biogenesis of DNA virus siRNAs by other DCLs (Blevins et al., 2006; Qu et al., 2008). In *Arabidopsis SE* encodes for a C_2H_2 – type zinc finger protein and act as a general regulator of miRNA levels (Lobbes et al., 2006; Yang et al., 2006). It co-localizes with DCL1 and HYL1 in nuclear dicing bodies (D-bodies) (Yang et al., 2006) and also with both subunits of Cap-binding Complex proteins (CBC20 and CBP80) (Raczynska et al., 2014), acting therefore, as bridge connecting the miRNA pathway and the spliceosome (Laubinger et al., 2008; Lobbes et al., 2006). This latter interaction, in addition, promotes the association with Ser5- and Ser2-phosphorylated RNA polymerase II (pol II) complexes regulating the transcription of mainly intronless genes (Speth et al., 2018). Recent findings have demonstrated the contribution of SE in remodeling of pri-miRNAs through the interaction with Chromatin Remodeling Factor 2 (CHR2) (Wang et al., 2018). In plants, both RNA transcription maturation and miRNA biogenesis are responsible for the determination of the proper level of particular miRNAs, their mRNA targets, as well as their response to environmental cues. Studies in *A. thaliana* have proposed SE as a positive regulator of plant defense either upon necrotrophic fungal infection (Voisin et al., 2009) or upon bacterial infection (Niu et al., 2016).

In our previous studies, we have demonstrated the implication of the RNA silencing pathway through DCL2, DCL3 and DCL4 in PSTVd pathogenicity (Dadami et al., 2013; Katsarou et al., 2016). Specifically, *N. benthamiana* knock-down (KD) plants with DCL4 suppression were found to positively affect PSTVd infectivity. Single suppression of DCL2 or DCL3 did not significantly affect PSTVd titer, while the combined action of DCL2/DCL3 was shown crucial for plant defense against PSTVd (Dadami et al., 2013; Katsarou et al., 2016). In this work, we aim to revisit the role of the miRNA biogenesis pathway on *Pospiviroidae* infectivity. Previous attempts to elucidate the role of DCL1 in viroid infection suggested that in DCL1 KD plants infection was less efficient than in WT (Dadami et al., 2013). However, in our system DCL1 KD plants had only a moderate DCL1 reduction, most likely due to the fact that DCL1 knock-out (KO) may be embryo-lethal (Qin et al., 2017; Schauer et al., 2002). In addition, we observed that there was a significant variability in viroid infection levels between individual plants which made the interpretation of DCL1i/PSTVd infectivity results difficult Dadami et al., 2013.

Here, in order to achieve significant miRNA pathway suppression and taking into account the embryonic lethality of DCL1 KO plants we included in our experimental set-up *N. benthamiana and N. tabacum* SE KD plants. Our data reveal that there is a strong reduction of *Pospoviroidae* titer in SEi *N. tabacum* and *N. benthamiana* as well as in DCL1i KD *N. benthamiana* lines. The above findings support the idea that both SE and DCL1 might act as positive factors of PSTVd infectivity.

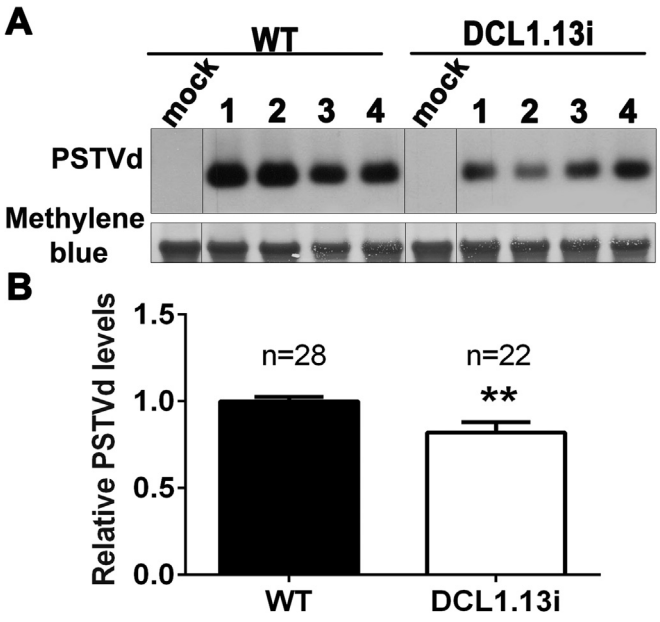

Fig. 1. PSTVd accumulation in *N. benthamiana* DCL1i lines. A. Northern analysis of total RNA for the detection of (+) PSTVd accumulation in WT and DCL1.13i plants. (-) PSTVd strand was used as a probe and methylene blue (total RNA) staining was used as loading control. **B.** Northern blot quantification analysis ''n" corresponds to the number individual plants analyzed. Unpaired Student *t*-test was performed with level of significance set as $p < 0.01$ (**). Standard error is depicted in graph.

2. Results

2.1. Infection of DCL1i plants with PSTVd by agroinfiltration

Based on the structural and functional evidence that indicate a possible connection between the miRNA pathway and viroid infectivity, we investigated the existence of such a link using previously described plants that suppress miRNAs. To this end, the *N. benthamiana* DCL1 RNAi KD transgenic line (DCL1.13i) that has been shown to reduce DCL1 expression by 37.2% was used (Dadami et al., 2013; Katsarou et al., 2016). In order to assess whether PSTVd infectivity is affected when the miRNA pathway is suppressed, wild type (WT) and DCL1i suppressed plants were inoculated by leaf infiltration with PSTVd^{NB} at the early stage of 4–6 leaves. Viroid inoculated *N. benthamiana* plants were grown in a greenhouse and 21 days post-inoculation (dpi) tissue was collected from three systemic, young leaves and used for total RNA extraction. Northern analysis for PSTVd was performed for five independent experiments and a total of 28 WT and 22 DCL1.13i plants (Fig. 1A), showing decreased PSTVd titer in all DCLi plants analyzed. Quantification of PSTVd titer revealed a moderate but significant reduction by 18% in DCL1.13i plants compared to WT (Fig. 1B). These results imply a positive correlation between DCL1 and miRNAs with PSTVd infectivity that prompted us to further investigate this phenomenon.

2.2. SERRATE suppressed plants

Since strong whole plant DCL1 suppression has not been possible, we opted for suppressing the miRNA pathway through another of its major components, SE. A single SE homologue was identified in *N. benthamiana* (Niben101Scf00862g00016.1) and *N. tabacum* (mRNA_112992_cdsmRNA). Genomic sequences available show 66% and 67% identity of the two sequences respectively at the protein level to *A. thaliana* SE (AT2G27100.1) (Fig. S1). Therefore, it was hypothesized that the SE homologue in these plants would have a crucial role in

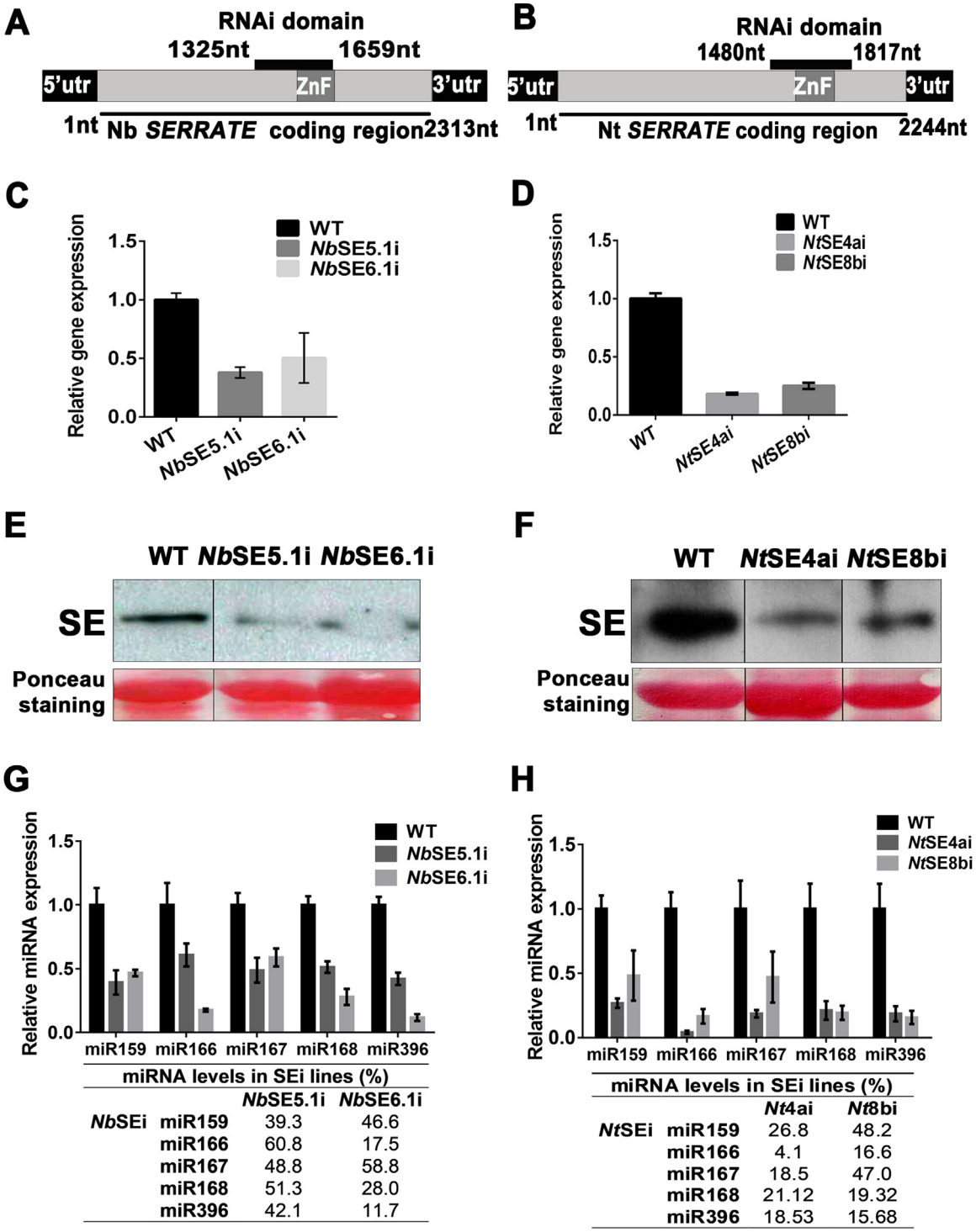

miRNA levels in SEi lines (%)

		*Nb*SE5.1i	*Nb*SE6.1i
*Nb*SEi	miR159	39.3	46.6
	miR166	60.8	17.5
	miR167	48.8	58.8
	miR168	51.3	28.0
	miR396	42.1	11.7

miRNA levels in SEi lines (%)

		*Nt*4ai	*Nt*8bi
*Nt*SEi	miR159	26.8	48.2
	miR166	4.1	16.6
	miR167	18.5	47.0
	miR168	21.12	19.32
	miR396	18.53	15.68

Fig. 2. Molecular characterization of *N. benthamiana and N. tabacum* SEi lines. A. Schematic representation indicating the part of the *N. benthamiana* and **B.** *N. tabacum* SE transcript targeted by the RNAi lines. **C.** qPCR for SE in *Nb*SEi and **D.** *Nt*SEi lines. **E–F.** Western blot analysis for the detection of SE using a SE-specific antibody. Total protein extract was used from young leaves of WT and **E.** *NbSEi* plants and **F.**WT and *NtSEi* plants. Ponceau staining was used to visualize the large subuit of Rubisco and served as the loading control. **G–H.** qPCR analysis of various miRNAs in **G.** *Nb*SEi and **H.** *Nt*SEi lines. Young leaves from 4, 5 week-old plants were used for the RNA preparation and the results were normalized to the value of the wild-type plants, whose value was arbitrarily fixed at 1. In **C–D** and **G–H**, 4 individual samples were used; standard error is depicted in graph.

miRNA biogenesis too. Based on studies in *Arabidopsis* showing that *SE* KO is embryo-lethal (Lobbes et al., 2006), we constructed transgenic *N. benthamiana* and *N. tabacum* plants that suppressed *SE* through RNAi. For *N. benthamiana*, a 334 bp *N. benthamiana* cDNA fragment, including a part of the characteristic Zinc-finger domain, was used as the RNAi target (Fig. 2A). For *N. tabacum a* 342 bp *Solanum lycopersicum*, Zinc-finger containing, cDNA fragment was used, sharing 93% identity with the *N. tabacum SE* cDNA (Fig. 2B). Based on BLASTn analysis, constructs for both *N. benthamiana* and *N. tabacum* were chosen to specifically target only SE sequences (not shown). We generated 11 *N. benthamiana* and 19 *N. tabacum* transgenic lines. Two lines from each species were further used in this study, (*Nb*SE5.1i and *Nb*SE6.1i of *N. benthamiana*,

*Nt*SE4ai and *Nt*SE8bi of *N. tabacum*). The degree of SE suppression was analyzed by quantitative PCR (qPCR) and was found to be 62.1% for *Nb*SE5.1i and 50.5% for *Nb*SE6.1i, compared to WT plants (Fig. 2C). Even more significant SE suppression was achieved in *N. tabacum* SEi transgenic lines (81.8% for *Nt*SE4ai and 75% for *Nt*SE8bi) (Fig. 2D), while the generation of siRNAs in these two *Nt*SEi lines was analyzed with northern hybridization (Fig. S2A). This SE suppression was also verified at the protein level for both *Nb*SEi (Fig. 2E) and *Nt*SEi lines (Fig. 2F) where SE protein levels were significantly reduced. In order to confirm the effect of SE suppression on miRNA biogenesis in *Nicotiana*, levels of various miRNAs were assessed by qPCR. In both *N. benthamiana* transgenic lines, miRNA accumulation for all miRNAs tested (miR159, miR166, miR167, miR168, miR396) was found significantly reduced, from 88.3% to 39.2%, compared to WT. Specifically, in line *Nb*SE5.1i, miRNA levels ranged from 39.3%, for miR159 to 60.8% for miR166 of the WT, while for the *Nb*SE6.1i line the miRNA levels ranged from 11.7% for miR396 to 58.8% for miR167 (Fig. 2G). Likewise, miRNAs analyzed in *N.tabacum* transgenic lines were strongly reduced from 51.8% to 95.9% compared to WT. Noticeably, in *Nt*SE4ai, miRNA levels ranged from 4.1% for miR166 to 26.8% for mir159 of the WT. For *Nt*SE8bi the levels of these miRNAs were 16.6% and 48.2%, respectively (Fig. 2H).

Next, we analyzed the phenotype of SEi produced lines. Both, *N. benthamiana* and *N. tabacum* SEi plants had reduced plant stature already from the juvenile stage that persisted throughout development (Fig. 3A, B). Leaves were more wrinkled, exhibiting partial loss of asymmetric differentiation and downward leaf curling, possibly as a result of partial loss of leaf asymmetry (Fig. 3C, D). Some *Nb*SEi plants exhibited also increased branching (Fig. 3E). At later stages of development phylotaxy was affected, especially in *Nt*SEi, plants and internode length was found significantly reduced (Fig. 3F). Flowering time was also affected in the SE mutants; WT plants flowered in our conditions on average 105 days post germination, while it took 146 days on average for *Nt*SE4ai plants and 129 days on average for *Nt*SE8bi plants to flower (Fig. S2B). In addition to the late flowering phenotype, 43% of *Nt*SE4ai plants never flowered, signifying the importance of SE in plant development. Nevertheless, the number of leaves produced before flowering was the same in WT and SEi lines (26 leaves on average) (Fig. S2C).

Additionally, we attempted to generate plants suppressed for both DCL1 and SE. To this end, we crossed a large number of *N.benthamiana* SEi to DCL1.13i plants but were unable to recover seeds although as described above, both lines had only partial suppression of the targeted gene. Fruit was set but went dark and necrotized few days after crossing without setting seeds. It should be noted that, both DCL1i and SEi *N. benthamiana* plants produce seeds upon self-pollination and upon crossing to WT although with lower efficiency.

Summarizing the above results, we generated *N. benthamiana* and *N. tabacum* SEi plants through RNAi. All selected lines are functional as they present reduced miRNA levels and distinct phenotypical characteristics. Therefore, we were confident that they represented a miRNA-suppressed system that could be used in viroid infectivity experiments

2.3. Infection of SEi plants with PSTVd by agroinfiltration

Similar to DCL1.13i plants, WT and SEi suppressed *N. benthamiana* and *N. tabacum* plants were PSTVd inoculated by leaf infiltration as described above followed by northern analysis. The experiment was repeated five times, for a total of 31 WT and 32 *Nb*SE5.1i plants. Analysis of representative plants is presented in Fig. 4A. Similar analysis was performed for the *Nb*SE6.1i transgenic line; the experiment was repeated two times, for a total of 14 WT and 22 *Nb*SE6.1i plants and a representative northern blot is depicted in Fig. 4B. Quantification of PSTVd titer in both *N.benthamiana* transgenic lines revealed a potent reduction in PSTVd levels compared to WT (Fig. 4C). Specifically, PSTVd levels were reduced by 57% and 54.4% in *Nb*SE5.1i and *Nb*SE6.1i lines respectively, compared to WT (Fig. 4C). Reciprocally, we tested the effect of PSTVd infection on SE levels by quantitative PCR. RNA was extracted from young systemic leaves 21 dpi with the $PSTVd^{NB}$ through agroinfiltration. When *Nb*SEi plants, either mock or PSTVd infected, were compared with the respective WT plants, a constant SE suppression was observed (Fig. 4D). In *Nb*SEi plants SE was reduced by 83.3% in mock plants and by 76.3% in PSTVd infected plants (Fig. 4D). This finding confirmed that SE was suppressed throughout the experiment. The above results were also supported by experiments carried out in *N. tabacum* SEi lines. More specifically, similarly to *N. benthamiana, N. tabacum* SEi plants were infected with PSTVd through agroinfiltration and young systemic leaves were analyzed by northern hybridization 21 dpi. All, 23/23 (100%) WT plants used were successfully infected with $PSTVd^{NB}$. However, only 15 *Nt*SE4ai plants were effectively infected from a total of 28 plants (53.57%) (Fig. 5A). A representative northern analysis of *Nt*SE4ai infected plants is shown in Fig. 5B. Similar were the results from three independent experiments for the *Nt*SE8bi line. 8 out of 21 plants (38.1%) were successfully infected, compared to 19/19 (100%) infected WT plants (Fig. 5C). A representative northern blot is depicted in Fig. 5D. The above data were collected from three independent experiments and quantification of PSTVd titer in infected *Nt*SE4ai and *Nt*8b1i plants showed a 35.1% and 69.4% reduction respectively, compared to WT (Fig. 5E). The reduced PSTVd titers in all lines analyzed in the above experiments suggests that SE suppression has adverse effects on PSTVd infectivity, which even leads to SEi plants resistant to viroid.

2.4. SE suppression affects also HSVd infectivity

In the course of analyzing the impact of SE suppression on PSTVd infectivity, we extended our analysis to *Hop stunt viroid* ($HSVd^{Y09352}$- Family: *Pospiviroid*, Genus *Hostuviroid*),(Daros and Flores, 2004; Kofalvi et al., 1997) from the same family, but classified to a different genus. We used WT and *Nb*SE5.1i plants which, similar to the PSTVd experiment, were infected by agroinfiltration and analyzed by northern hybridization for HSVd accumulation, 21 dpi. As presented in Fig. 6A, HSVd accumulated at significantly lower levels in SEi suppressed plants. Quantification of all infected *Nb*SEi plants showed a 72.8% reduction of HSVd titer compared to WT (Fig. 6B). The experiment was repeated three times for a total of 56 WT and 41 *Nb*SE5.1i plants. The above findings indicate that the effect of SE suppression have significant consequences for both viroid species analyzed, implying a general role of SE in pospiviroids' infectivity.

2.5. Time-course analysis of PSTVd infection in SEi plants

In order to assess whether the effect of SEi suppression on viroid titer affected primarily the establishment of infection or maintenance and systemic spread, we analyzed infection: 1) in the infiltrated tissue soon after infection (5 dpi in infiltrated area) and, 2) in systemic tissues at different time points. We reasoned that, by analyzing the course of infections in systemic leaves we can assess whether in SEi plants the viroid has the potential to eventually reach titer similar to WT albeit later. To address this ability of viroid to establish infection in SEi plants, we infected WT and *Nb*SE5.1i plants with $PSTVd^{NB}$ and its titer was analyzed by northern blot at 5 dpi using RNA from the agroinfiltrated area, as shown in Fig. 7A. Quantification of PSTVd levels revealed a 67.5% reduction compared to WT, already 5 dpi, suggesting that the establishment of viroid infection is less efficient in SEi plants (Fig. 7B). Similar results were obtained from three independent experiments for a total of 20 WT and 17 SEi plants. For the maintenance and systemic spread time-point analysis, a pool of two systemic leaves were analyzed by northern hybridization at 7, 14, 21, 28, and 35 dpi. We found viroid titer to remain continuously reduced in SEi plants compared to WT

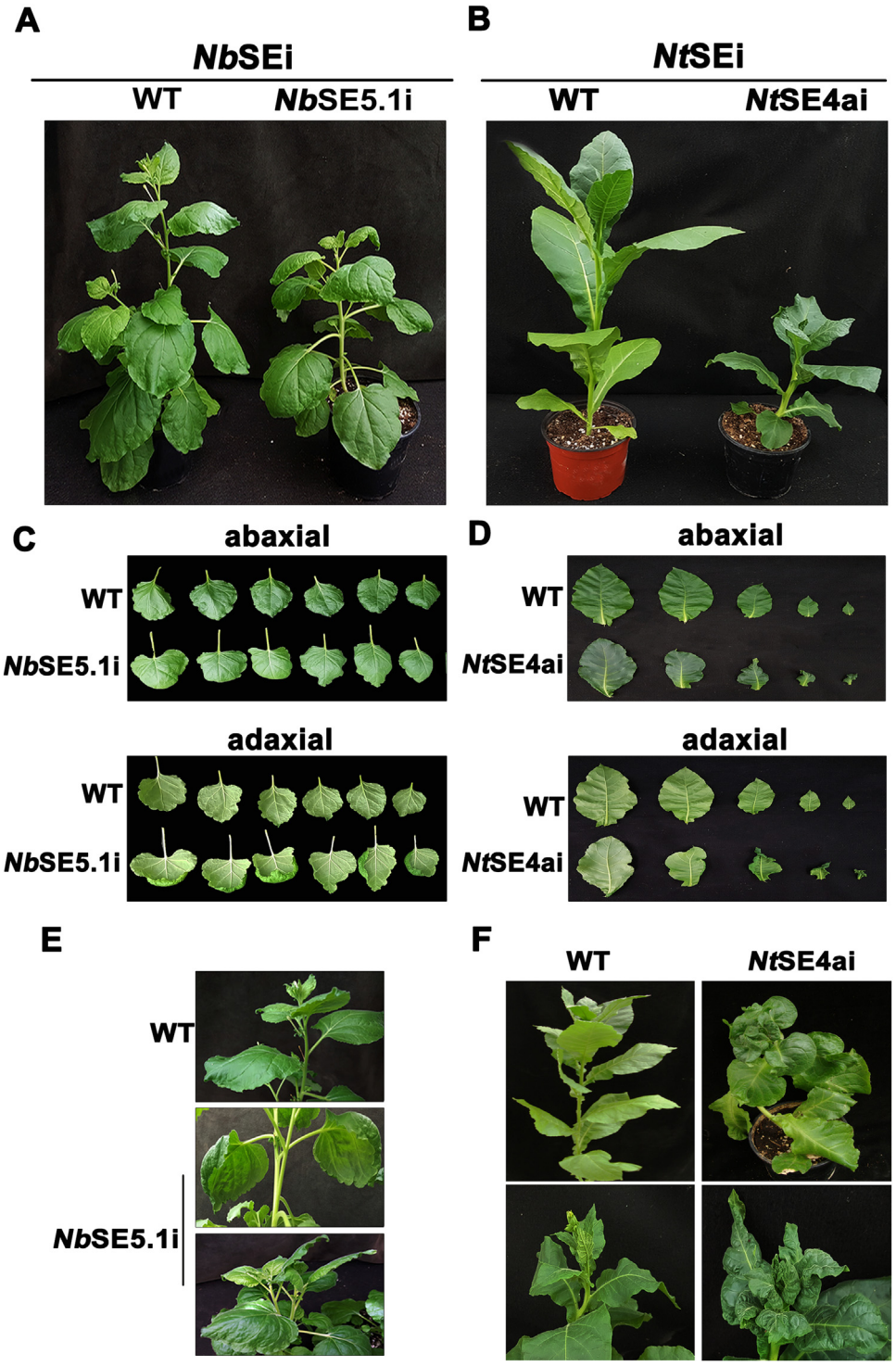

Fig. 3. Phenotypes of *N. benthamiana* and *N. tabacum* SEi lines. A. Phenotypes of 3-month-old WT, *N. benthamiana* and **B.** *N. tabacum* SEi plants. **C-D.** Images of abaxial and adaxial individual leaves of WT, **C.** *N. benthamiana* and **D.** *N. tabacum* SEi plants aged of 3 months. **E–F**. Images of *Nb*SEi plants **E.** and *Nt*SEi plants **F.** showing developmental abnormalities compared to WT.

plants, at all time point analyzed (Fig. 7C). The experiment was repeated at least two times with a minimum of 5 plants in each experiment. The above results indicate that SE suppression affects PSTVd accumulation throughout infection, although its role may be crucial at the initiation of infection.

2.6. Effect of SEi suppression on PSTVd replication is not supported

We reasoned that the reduced PSTVd infectivity in SEi plants might be a result of aberrations in PSTVd replication. In order to check this hypothesis, we probed for accumulation of replication intermediates ((-) strand viroid RNAs) assuming that aberrations in band profiles may indicate replication abnormalities. WT & SEi plants, 21 dpi were analyzed by northern hybridization and no significant differences were

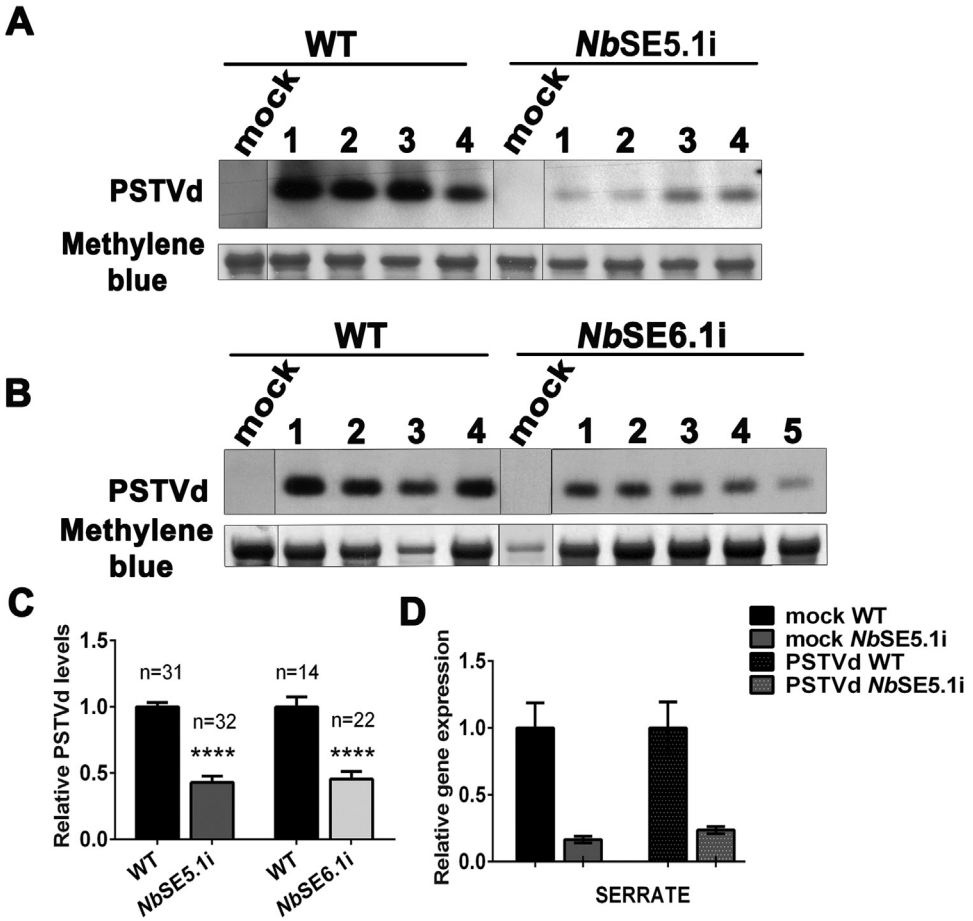

Fig. 4. PSTVd accumulation & *SERRATE* mRNA analysis in *N. benthamiana* SEi plants. Northern analysis of total RNA for the detection of viroid RNA from WT and SEi plants. Analysis of (+) PSTVd accumulation in **A.** *Nb*SE5.1i and **B.** *Nb*SE6.1i lines. (-) PSTVd was used as a probe and methylene blue (total RNA) staining was used as loading control. **C.** Graphical representation of northern blot quantification analysis. ''n'' corresponds to individual plants analyzed. Unpaired Student *t*-test was performed with the level of significance set as $p < 0.0001$ (****). **D.** qPCR analysis for SE mRNA expression in mock and PSTVd infected *Nb*SE5.1i plants. The results were normalized to the corresponding values of the WT mock and PSTVd infected plants whose value was arbitrarily fixed at 1.

observed in the profile of intermediate RNAs. Thus, it is unlikely that replication hindrance plays a major role in the reduced PSTVd titer in SEi plants (Fig. S3).

2.7. Strong reduction of viroid infectivity in mechanically inoculated SEi plants

Since the establishment of infection is significantly affected in SEi plants, we then asked whether the method used for viroid inoculation was critical in the effect observed in these plants, leading indirectly to reduced establishment of infection. To this end, instead of agroinfections we mechanically inoculated WT and *Nb*SE5.1i plants using sap from already PSTVd infected WT plants. Samples collected at 28 dpi were analyzed for PSTVd by northern hybridization. We found that using mechanical inoculation the effects of SE suppression were even more pronounced than when using the agroinfection method: only 2 out of 24 SEi plants (8.3%) unlike all 24 out of 24 WT plants (100%) were infected (Fig. 8Ai). A representative northern is shown in Fig. 8Aii, while, quantification of PSTVd titer in infected plants showed 64.8% PSTVd reduction (Fig. 8Aiii). Analysis of the infection at a later time point (42 dpi) showed very similar results. 4 out of 12 SEi plants analyzed (33.3%) were infected (Fig. 8Bi, ii, E) and had a 30.4% reduction in viroid titer (Fig. 8Biii), verifying the strong effect of SE suppressed plants on mechanical infection of PSTVd. The above results suggest that there is a positive correlation between SE levels and PSTVd infectivity, and this effect was even more pronounced when plants where inoculated mechanically with infectious sap.

3. Discussion

RNA silencing plays a key role in modulating many host – pathogen interactions (Ruiz-Ferrer and Voinnet, 2009). The distinctive characteristics of viroids and their capacity to induce RNA silencing responses (Itaya et al., 2001; Papaefthimiou et al., 2001; Tabler and Tsagris, 2004), have raised questions regarding their ability to evade plant responses without producing their own proteins. Previous studies by us and others have described the interplay between viroids with the antiviral and methylation related silencing pathways through the effects of DCL2/DCL4, DCL3 and Argonautes on viroid infectivity (Dadami et al., 2013; Katsarou et al., 2016; Minoia et al., 2014; Torchetti et al., 2016).

Here we revisit the interaction between miRNA biogenesis pathway and *Pospiviroidae* family viroids. Structural and functional similarities between miRNA precursors and viroids have led to suggestions that vd-sRNAs may function similar to miRNAs and could target host genes inducing disease symptoms (Markarian et al., 2004; Papaefthimiou et al., 2001; Wang et al., 2004). Equivalently to virus induced differentiation in host gene expression (Bazzini et al., 2007; Cillo et al., 2009), viroid induced changes in host homeostasis could generate a more favorable environment for viroid infection (Itaya et al., 2002; Wang et al., 2011). These changes may concern host genes misexpression (Navarro et al., 2012b) and differential miRNA levels (Diermann et al., 2010; Owens et al., 2012) which in turn regulate several hormone-signaling pathways, like auxin, brassinosteroid (BR) and giberellin (GA) response pathways (Owens et al., 2012; Zheng et al., 2017).

Unlike the suppression of DCL2, 3 and 4, which was very efficient through RNAi in *N. benthamiana*, even when suppressed simultaneously, we have been unable to generate viable plants with very strong DCL1 suppression (Dadami et al., 2013). This is in agreement with other reports in *A. thaliana* (Schauer et al., 2002) and *N. benthamiana* (Qin et al., 2017) where plants with strong DCL1 repression where shown to be embryo-lethal. In order to circumvent this, we opted to

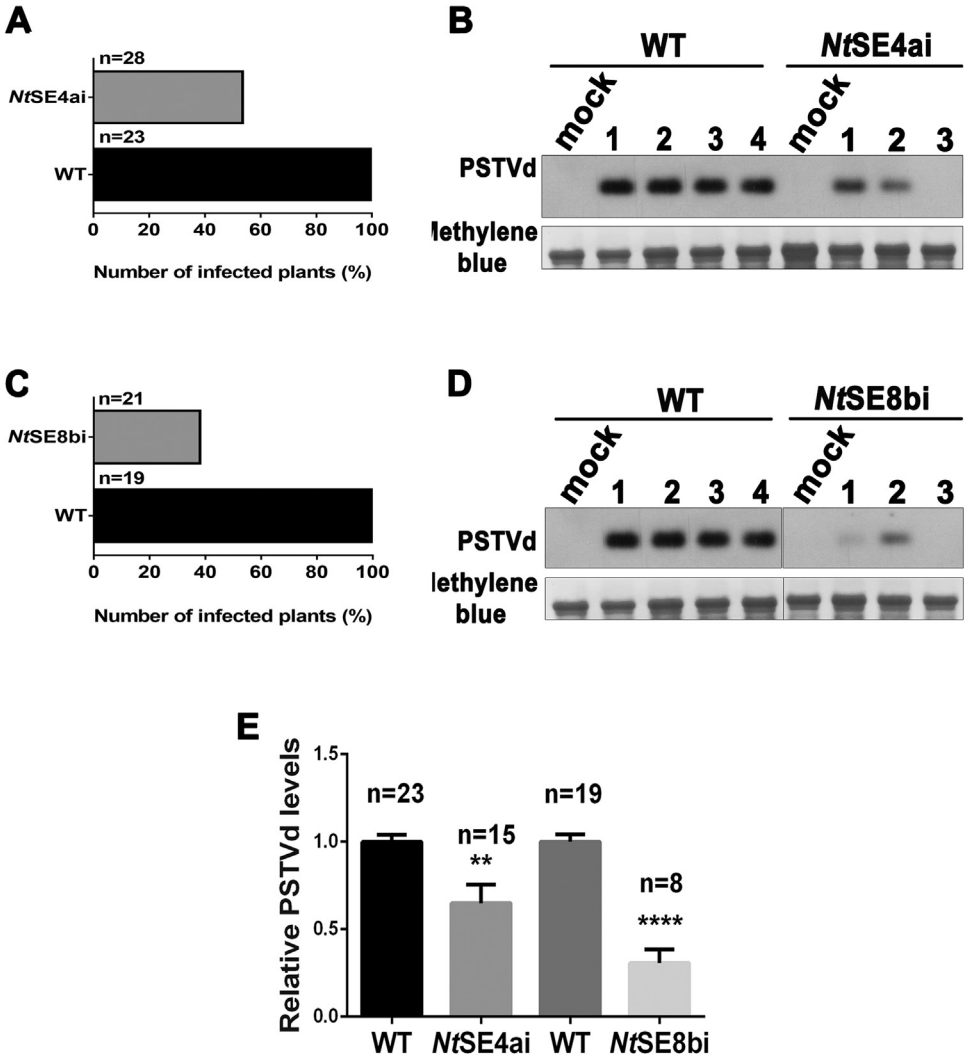

Fig. 5. PSTVd accumulation in *N. tabacum* SEi plants. Northern analysis of total RNA for the detection of (+) PSTVd in WT and SEi plants, as described in Fig. 4**A. A, C** Illustration of the percentage of successfully infected plants on the total of used plants **A.** of *Nt*SE4ai and **C.** *Nt*SE8bi plants. **B, D.** Representative northern blots 2I dpi of **B.** *Nt*SE4ai and **D.** *Nt*SE8bi plants. Methylene blue (total RNA) staining was used as loading control. **E.** Graphical representation of northern blot quantification of viroid titer of both *Nt*SE4ai and *Nt*SE8bi lines. ''n'' correspond to individual plants analyzed. Unpaired Student *t*-test was performed with the level of significance set as $p < 0.01$ (**) and $p < 0.0001$ (****) for *Nt*SE4ai and *Nt*SE8bi respectively.

suppress the miRNA pathway through another major component of this pathway, SE. Specific SE mutations have been previously described in *Arabidopsis* as being embryo – lethal under some environmental conditions, underlining the importance of the SE and miRNA regulation throughout plant development (Grigg et al., 2005; Lobbes et al., 2006). Nevertheless, we managed to suppress SE up to 62% in *N. benthamiana* and even 82% in tobacco indicating a higher tolerance to SE suppression than DCL1 suppression. There are at least two possibilities for this difference: either DCL1 is essential in more events in early development, or the essential amount of protein requested is larger for DCL1. It is not possible at present to distinguish between these two possibilities. Our inability to obtain seedlings from the SEixDCL1i (and reciprocal) crosses suggests that the strong SE reduction along with the most detrimental effects of DCL1 suppression, make it difficult to generate double SEi and DCL1i *N. benthamiana* plants.

The divergent phenotypes of SEi plants are indicative of the role of *SE* in organogenesis and plant development. Both *N. benthamiana* and *N. tabacum* SEi plants exhibit similar phenotypic characteristics in plant and leaf development. Additionally, in *N.tabacum* a very late flowering or even no flowering phenotype was observed. All SEi plants analyzed, exhibited reduced SE levels which also varied between individual lines. Nevertheless, we cannot not fully relate the expression levels with phenotypes, as was also discussed in the case of *Arabidopis* SEi mutants (Prigge and Wagner, 2001). The significant lower miRNA levels in all plants examined, which are much lower in *N. tabacum* SEi plants, are possibly responsible for such phenotypes, without excluding the possibility that other factors including mis-spliced growth related genes having an effect.

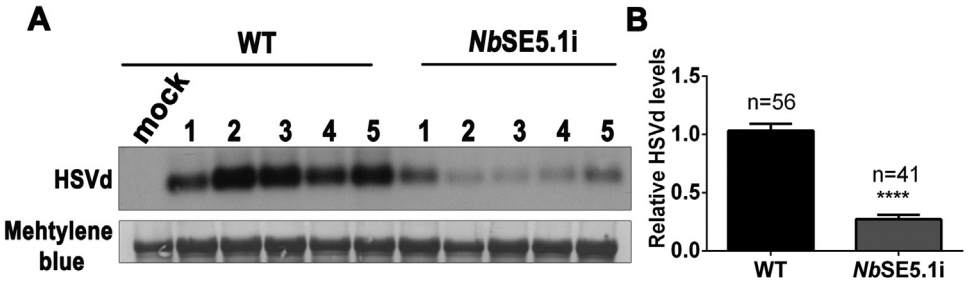

Fig. 6. HSVd accumulation in *N. benthamiana* SEi lines. A. Northern blot analysis for the detection of (+) HSVd in WT and *Nb*SE5.1i plants. Methylene blue (total RNA) staining was used as loading control. **B.** Graphical representation of viroid RNA signal. ''n'' correspond to individual plants analyzed. Unpaired Student *t*-test was used with the level of significance set as $p < 0.0001$ (****).

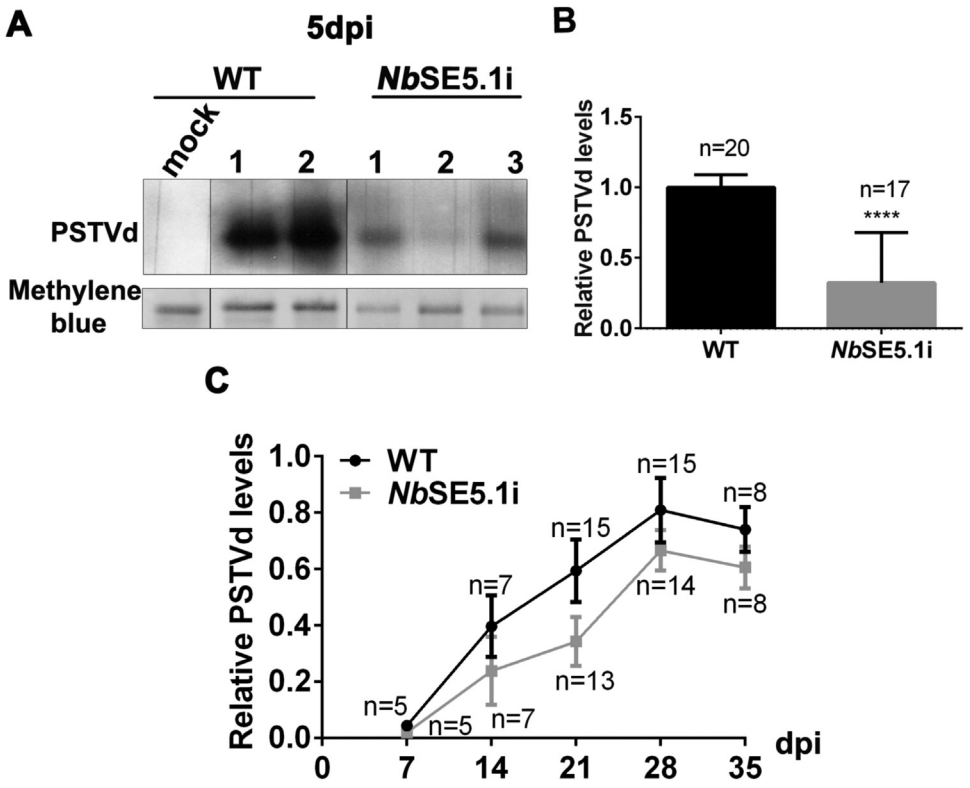

Fig. 7. Time course PSTVd accumulation in *N. benthamiana* SEi line. A. Northern blot analysis of total RNA for the detection of viroid RNA from WT and *Nb*SEi plants, 5 dpi in the agroinfiltrated area. Methylene blue staining was used as loading control. **B.** Graphical representation of viroid RNA signal. ''n'' correspond to individual plants analyzed. Results were analyzed with unpaired Student *t*-test, and the level of significance was set as $p < 0.0001$ (****). **C.** Graphical representation of viroid RNA signal 7, 14, 21, 28 and 35 dpi based on northern hybridization results. ''n'' correspond to individual plants analyzed. The graph depicts mean values (with standard error) of PSTVd levels.

In order to assess the role of the miRNA pathway on *Pospiviroid* infectivity, we investigated PSTVd accumulation in both DCL1 and SE suppressed plants. Previous experiments on the effect of DCL1 suppression on viroid accumulation suffered from the high variability of infection in individual DCL1 plants. We had reasoned that this may have been due to developmental and other differences observed between individual DCL1i plants as a result of miRNA dis-genesis (Dadami et al., 2013). Here, the use of younger and presumably less divergent plantlets, lead to improved uniformity of infections. In DCL1.13i *N. benthamiana* plants, we found moderate but significant reduction of

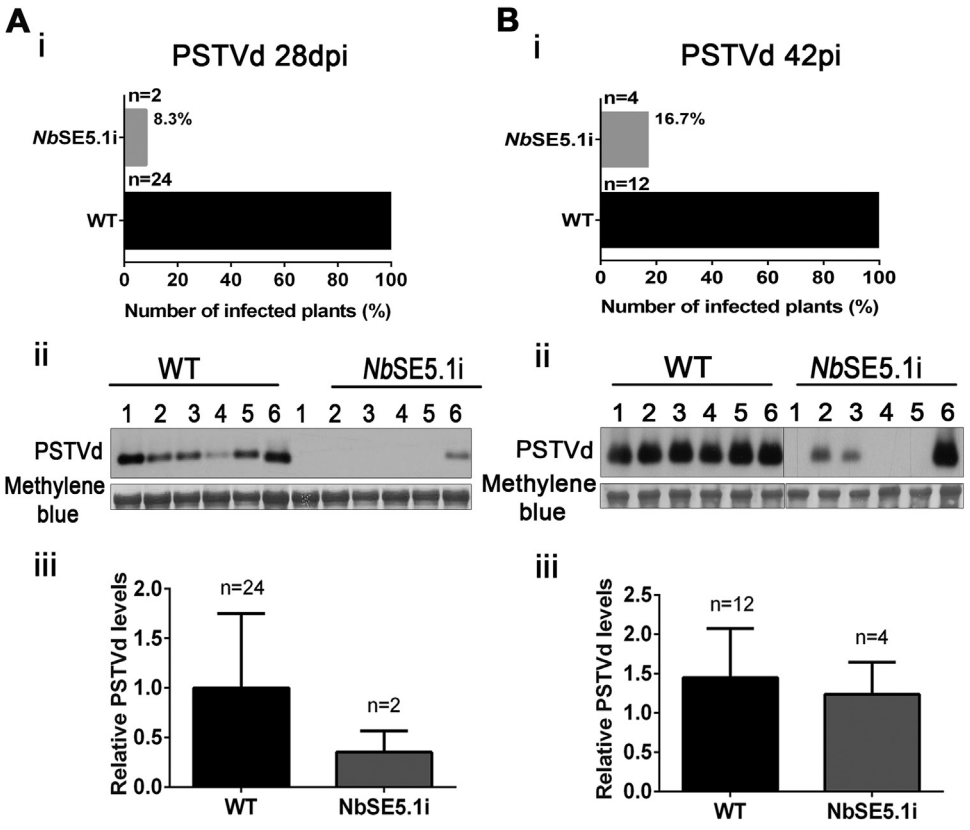

Fig. 8. PSTVd titer of mechanically infected plants. WT and *Nb*SE5.1i plants were mechanically infected with PSTVd sap and analyzed **A**. 28 dpi and **B**. 42 dpi. **Ai, Bi,** Illustration of the percentage of successfully infected plants on the total of used plants **Ai.** 28 dpi and **Bi.** 42 dpi. **Aii, Bii.** Northern analysis at **Aii.** 28 dpi and **Bii.** 42 dpi. Methylene blue (total RNA) staining was used as loading control. **Aiii**, **Biii**, quantification graph of viroid titer **Aiii.** 28 dpi and **Biii.** 42 dpi ''n'' correspond to individual plants analyzed. The graphs depict mean values (with standard error) of PSTVd levels.

PSTVd titer by 18% compared to WT. We presume that the moderately lower viroid titer compared to WT infected was due to the modest DCL1 suppression of the RNAi plants. In contrast northern analysis of SEi plants revealed strong reduction in PSTVd titer, in both *N. benthamiana* and *N. tabacum*. This greater impact on PSTVd infectivity might be due to the more effective suppression of SE compared to DCL1. It cannot be excluded nevertheless that, SE may affect viroid infectivity also through its involvement in transcription and RNA processing events. We observed some variability of PSTVd infection between individual plants of all SEi - miR deficient transgenic lines. We reasoned that this variance may be related to some stochasticity in the effects of miRNA depletions on plant development while we cannot rule out environmental effects. This phenomenon was more pronounced in *N. tabacum* that had the strongest miRNA suppression where only 50.9% of both *Nt*SE4ai and *Nt*SE8bi were finally found infected. Furthermore, HSVd infection of SEi plants suggests that the observed phenomenon could be a general feature of *Pospiviroidae*.

Analysis of PSTVd infection in the infiltrated tissue soon after the infection as well as in systemic leaves at different time points revealed the crucial role of SE in the onset of PSTVd infection. However, the steadily lower viroid titer throughout the infection suggest that SE positively affects PSTVd accumulation and also the maintenance of infection. Further, evaluation of (-) strand viroid RNA at late stage of infection, did not reveal significant differences in the profile of intermediate RNAs, implying that PSTVd titer decrease might be independent of an effect on replication intermediates. Additional analysis however, will be required to elucidate this effect.

The effect of SE suppression on viroid infectivity was even more pronounced when we used mechanical inoculations to infect the plants (8.3% and 33.3% of plants analyzed were infected at 28 and 42 dpi respectively). This could be due to the effect of SE suppressed plants in factors that involve in mechanical infection and are different from those of agroinfiltration, such as the introduction of the viroid to the cell and then translocation to the nucleus, which in the case of agroinfection is accommodated by the bacterium. Moreover, recent findings in Arabidopsis associate SE with cell wounding response proteins (Speth et al., 2018), which also could be affected in SEi plants.

In this study we aimed to understand the interplay between the factors of miRNA biogenesis pathway and infectivity of *Pospiviroidae* viroids. We show that DCL1 as well as SE, an important factor of miRNA biogenesis, positively affect viroid (PSTVd and HSVd) infectivity. Viroid titer is reduced in DCL1i and SEi plants, and this decrease is more pronounced upon mechanical PSTVd infection. The results presented here are in agreement to a possible role of the miRNA pathway in viroid infectivity. More studies, however, are required in order to elucidate which is the mechanism behind this effect.

4. Materials and methods

4.1. Plasmid construction

For the generation of *N. benthamiana* SE suppressed lines via RNA silencing, a 334 bp cDNA fragment, containing a large part of ZnF domain (Fig. 2A), which is specific only for SE, was amplified by PCR with specific primers: (SEhpN.b F(up): 5′-AGAATTCCCTATCTGTGGCGCA TTC-3′ and SEhpN.b R (low):5′-TCTCGAGATGGACAAATTCGGC AGC-3′; restriction sites underlined). The amplified fragment was digested with *Eco*RI / *Xho*I restriction enzymes and inserted in pENTR™3C (Invitrogen) donor vector at the respective plasmid sites. With the Gateway® cloning technology the hairpin fragment was subcloned in pK7GWIWG(I) destination vector to create the pK7-35S: *Nb*SEi construct.

For the generation of *N. tabacum* SE suppressed lines the construct was designed based on *Solanum lycopersicum* sequence sharing 93% identity with the *N. tabacum SERRATE* cDNA equivalent (Fig. S1). A 342 cDNA fragment, containing the ZnF domain (Fig. 2B), which is specific only for SE,was amplified by PCR with specific primers: (Sl. SEhairpinF: 5′-CCGGATCCCCGAAGCCTTAGATCCC-3′ and Sl. SEhairpinR: 5′-CCCT CGAGCGCCATTAGCACGTCC-3′; restriction sites underlined). The amplified fragment was digested with *BamH*I / *Xho*I restriction enzymes and inserted in pENTR™3C (Invitrogen) donor vector at the respective plasmid sites. With the Gateway® cloning technology the hairpin fragment was then subcloned to pK7GWIWG(I) destination vector to create the pk7-35S: *Nt*SEi construct.

4.2. Plant transformation

Transgenic plants were constructed according to Horsch et al. (1985), leaf disc transformation protocol, with minor modifications as described previously (Kalantidis et al., 2002). Briefly, *Agrobacterium tumefaciens* C58C1 strain carrying the appropriate construct was incubated at 28 °C for 36 h. After centrifugation, the cells were dissolved in 20 ml MS solution (Murashige and Skoog, 1962). Young *N. benthamiana* leaves were sterilized in 10% chlorine/0.1% Tween solution for 10 min and washed with water 3 times. After incubation of cut leaf discs of 5 mm diameter in resuspension solution of *Agrobacteria* for 20 min, they were rinsed in MS solution and transferred in Petri dishes with MS media, upside down. Post 48 h, leaf discs were rinsed with MS solution, containing cefotaxime bactericidal to 250 μg/ml final concentration and transferred in MS media containing 0.8 mg/ml 1.6 benzyl-aminopurine (BAP), 0,1 mg/ml naphthalene acetic acid (NAA) and the appropriate antibiotics. Substrate changes were made every 3–4 days for the first 20 days and then every 2 weeks. Once the calli were formed, they were transferred to bigger pots, while when the seedlings are formed, they are cut off and transferred to non-hormonal nutritional rooting media until roots were formed roots and are ready to be transported to soil in the stable conditions of the glasshouse.

4.3. Plant materials and growth conditions

N. benthamiana and *N. tabacum* plants, WT and SE suppressed plants were used. For the selection of transgenes, seeds were plated under aseptic conditions in Petri dishes containing MS media (Murashige and Skoog, 1962) with the suitable antibiotic. Plates were transferred in growth chamber under long day conditions (16 h light/8 h dark, temperature 22 °C, humidity 40%). After germination and selection of transgenes, plants were transferred in soil (2:1:0.5, humo: peat: perlite) and grown in glasshouse in the same conditions.

Experiments were conducted in homozygous *N. benthamiana* plants in T3 generation and *N. tabacum* plants T4 generation. Also, *N. benthamiana* plants which suppress DCL1 were used in T7 generation (Dadami et al., 2013).

4.4. Viroid infections

Viroid inoculation performed in young plants at the age of 4–6 leaves, using two different types of infections.

For infection through agroinfiltration, the *Agrobacterium tumefaciens* GV3101 strain carrying an infectious PSTVd dimer (PSTVd^{NB} – AJ634596) (Qi et al., 2004) kindly provided by Dr. De Alba and Dr. Flores (Institute for Cellular and Molecular Plant Biology—IBMCP) was used or *A. tumefasciens C58C1* strain containing plasmid pCdHSVd (HSVdY09352) (Daros and Flores, 2004). Agroinfiltration was conducted exactly as described before (Kościańska et al., 2005).

For mechanical infection, plants were inoculated with infectious sap from *N. benthamiana*, using carborundum (Prolabo, VWR), as described before (Tabler and Sänger, 1984). Specifically, infected *N. benthamiana* leaf tissue was homogenized in 50 mM $NaPO_4$ buffer, pH 6.8 with 1:4 ratio (tissue: buffer). Fifty microliters of the infectious homogenate were used to infect each individual *N. benthamiana* leaf.

In both ways of infections, two leaves of each plant were inoculated. Young, systemic leaves were collected at 21 dpi. For time point

experiments, tissue was collected from 7 days post infection and every 7 days, up to 35 dpi.

4.5. RNA extraction

Total RNA was extracted from young leaves as described before (Dadami et al., 2013). Briefly, healthy and infected leaf samples were homogenized under liquid nitrogen and then RNA extraction buffer (38% saturated phenol, 0.8 M guanidine thiocyanate, 0.4 M ammonium thiocyanate, 0.1 M sodium acetate, 5% glycerol) was added in 10:1 ratio (RNA extraction : tissue). After vortexing, the mix was incubated in RT for 5 min and then centrifuged in 12.600 rpm for 10 min, at 4 °C. The supernatant was transferred in a new tube and 0.2 volumes of chloroform are added. The mix was incubated in RT for 10 min and centrifuged in 12.600 rpm for 10 min, at 4 °C. The supernatant was transferred in a new tube and precipitation was achieved by adding 0.5 volumes of isopropanol, incubation for 1 h at − 80°C and centrifugation for 30 min at 4 °C. Pellet was washed with 70% v/v ethanol and diluted in 50 μl ddH_2O.

4.6. Northern blot hybridization

Northern blot analysis for large RNAs was done as previously described (Katsarou et al., 2016; Mermigka et al., 2016). Briefly, 5 μg of total RNA, were analyzed in denaturating agarose gel (1.4% agarose, 0.7% formaldehyde, 1 × MOPS, 7 μg ethidium bromide per 100 ml gel), in denaturating buffer (0.7% formaldehyde, 1 × MOPS). After equilibration of gel in 2 × SSC for 20 min, total RNA was transferred onto 0.45 μm nylon membrane (NytranN, Whatman, GE healthcare) in 10 × SSC via capillary transfer, for 16–20 h. RNAs were crosslinked with UV radiation (Stratalinker, Stratagene, USA) of 1200 μJ cm^{-2} total energy.

Detection of PSTVd transcripts was performed as described before (Katsarou et al., 2016), RNA (-) DIG labelled probe (DIG RNA labelling mix, Roche) was produced by T7 transcription from *Hind*III- cut pHa106 plasmid (Tabler et al., 1992) and hybridization was performed overnight at 65 °C in hybridization buffer (5 × SSC; 1% SDS; 1 × Denhardt's; 250 mg/ml tRNA; 50% formamide). Then, three washes were made, two with 2 × SSC/0.2% SDS for 30 min and one with 1 × SSC/0.2% SDS for 15 min, all at 65 °C. CDP -star (Roche Diagnostics) was used for the detection according to the manufacturer instructions. Band intensity was quantified with the software Quantity One 4.4.1 (Biorad, USA) and values were normalized to leaf samples for each plant using ribosomal RNA (25S rRNA) as a control and then to the WT values. Statistical analysis was performed using GraphPad Prism 6 software (GraphPad software Inc).

4.7. Reverse transcriptase and quantitative PCR

For gene expression analysis the quantitative PCR (qPCR) was used. 3 μg of total RNA were treated with DNaseI (Roche). After phenol: chloroform treatment RNA was converted to cDNA using Minotech RT and oligo dT primer (Invitrogen) according to manufacturer instructions. After analyzing cDNAs for gDNA contamination by amplifying a reference gene, 1:5 dilution was used for gene amplification with KAPA SYBR® FAST qPCR Kit (KapaBiosystems) on the CFX ConnectTM Real-Time PCR detection System (Bio-Rad). Annealing and extension were carried out in one step at 60 °C or 62 °C for 20 s depending on the primers (Table S1). Samples were processed in triplicates and efficiency of each primer set was calculated using plasmid standard curves in the range of 90–110%. The L23, PP2A and UBI3 RNA were used as loading control in order to have a $p < 0.05$ using BestKeeper algorithm (Andersen et al., 2004). The results were normalized to the value of the wild-type plants, whose value was arbitrarily fixed at 1. Expression analysis was performed using the Pfaffl method (Pfaffl et al., 2004). All primers and annealing conditions are listed in Table S1 (Kotakis et al., 2010; Liu et al., 2012)

For miRNA analysis, 500 ng of total RNA was treated with *DNAseI* (Roche) and purified with phenol: chloroform technique. DNase-treated RNA was converted to cDNA using Minotech RT, dNTPs (Invitrogen) and 0.5 μM of the reverse RT primers designed according to (Varkonyi-gasic et al., 2007) (Table. S1). The mix was heated at 80 °C for 5 min, followed by addition of the reaction buffer in 1 × final concentration, 5 mM DTT and 40 units RRI (Takara). The mix was then incubated for 30 min at 16 °C, 60 min at 55 °C and 15 min at 72 °C. cDNA was used in 1:20 dilution for miRNA amplification as described above. Annealing and extension were carried out in one step at appropriate Tm (Table S1). Samples were processed in triplicates and as internal reference, three different nucleolar small RNAs (U1, U4 and U6) which are stable in the tested conditions according to BestKeeper algorithms (Andersen et al., 2004), were used. All Reverse transcriptase reactions, including no-template controls and RT minus controls, were run in duplicates. Expression analysis was performed using the Pfaffl method (Pfaffl et al., 2004). All primers and annealing conditions are listed in Table S1.

4.8. Protein extraction

For total protein extraction, young leaves were homogenized in liquid nitrogen and protein extraction buffer (100 mM Tris-Cl pH = 8, 200 mM NaCl, 1 mM EDTA, 3 mM $MgCl_2$, 1 mM DTT, 10% glycerol, 10 μg/μl PMSF and Complete Protease Inhibitor Cocktail Tablets (Sigma)) was added in 5 : 1 ratio (buffer : tissue). After shaking vigorously by vortex for 1–2 min and cooling on ice for 30′, the mixture was centrifuged for 30′ at 4 °C and 12.000 rpm. The supernatant was transferred to a new tube for further use after adding 6 × loading dye.

4.9. Western blot assay

Total proteins (100 mg) were fractionated in 8% SDS-PAGE mini-gel (Bio-Rad), and blotted to nitrocellulose membrane (ProtranN, Whatman) by wet transfer in 25 mM Tris, 150 mM glycine, 20% methanol at 310 mA, for 1.5 h at 4 °C. For the analysis with SE-specific antibody (Agrisera), the membrane was blocked in TBS-T buffer (200 mM Tris-HCl pH 7.5, 1.5 M NaCl, 0.1% Tween-20) containing 3% milk at room temperature for 1 h. After two washes of 5 min with TBS-T, membrane was incubated with antibody diluted 1:3000 in TBST containing 1% milk for 1 h at room temperature. Three washes of 5 min with TBS-T were followed by the addition of goat anti-rabbit IgG alkaline peroxidase-conjugate (Promega) diluted (1:10,000) in TBS-T containing 1% milk for 1 h at room temperature. After three washes of 5 min with TBS-T, signals were detected using the SuperSignal West Pico Chemiluminescent Substrate (Thermo Scientific).

Acknowledgments

This work was supported by a grant of the General Secretary for Research and Technology of Greece, Infrastructures support program [MIS5002803] "PlantUP". K. Katsarou received a grant by the Greek State Scholarship Foundation (IKY) [MIS5001552—Human Resources Development Program, Education and Lifelong Learning, for the Strengthening of Post-Doctoral Research, co-financed by the European Social Fund (ESF) and the Greek government.

Conflict of interest

The authors have declared that they have no competing interest.

Appendix A. Supplementary material

Supplementary data associated with this article can be found in the online version at doi:10.1016/j.virol.2018.12.011.

References

Ahmed, Hadidi, Ricardo, Flolres, Randless, John W., J.S.S, 2014. Viroids. https://doi.org/10.15713/ins.mmj.3.

Andersen, C.L., Jensen, J.L., Ørntoft, T.F., 2004. Normalization of real-time quantitative reverse transcription-PCR data: a model-based variance estimation approach to identify genes suited for normalization, applied to bladder and colon cancer data sets. Cancer Res. 64, 5245–5250.

Baulcombe, D., 2004. RNA silencing in plants. Nature 431 (7006), 356–363. https://doi.org/10.1038/nature02874.

Bazzini, A.A., Hopp, H.E., Beachy, R.N., Asurmendi, S., 2007. Infection and coaccumulation of tobacco mosaic virus proteins alter microRNA levels, correlating with symptom and plant development. Proc. Natl. Acad. Sci. USA 104, 12157–12162. https://doi.org/10.1073/pnas.0705114104.

Blevins, T., Rajeswaran, R., Shivaprasad, P.V., Beknazariants, D., Si-Ammour, A., Park, H.S., Vazquez, F., Robertson, D., Meins, F., Hohn, T., Pooggin, M.M., 2006. Four plant dicers mediate viral small RNA biogenesis and DNA virus induced silencing. Nucleic Acids Res. 34, 6233–6246. https://doi.org/10.1093/nar/gkl886.

Bologna, N.G., Voinnet, O., 2014. The diversity, biogenesis, and activities of endogenous silencing small RNAs in *Arabidopsis*. Annu. Rev. Plant Biol. 65, 473–503. https://doi.org/10.1146/annurev-arplant-050213-035728.

Bouché, N., Lauressergues, D., Gasciolli, V., Vaucheret, H., 2006. An antagonistic function for Arabidopsis DCL2 in development and a new function for DCL4 in generating viral siRNAs. EMBO J. https://doi.org/10.1038/sj.emboj.7601217.

Cillo, F., Mascia, T., Pasciuto, M.M., Gallitelli, D., 2009. Differential effects of mild and severe *Cucumber mosaic virus* strains in the perturbation of microRNA-regulated gene expression in tomato map to the 3′ sequence of RNA 2. Mol. Plant-Microbe Interact. 22, 1239–1249. https://doi.org/10.1094/MPMI-22-10-1239.

Dadami, E., Boutla, A., Vrettos, N., Tzortzakaki, S., Karakasilioti, I., Kalantidis, K., 2013. Dicer-like 4 but not Dicer-like 2 may have a positive effect on potato spindle tuber viroid accumulation in nicotiana benthamiana. Mol. Plant 6, 232–234. https://doi.org/10.1093/mp/sss118.

Daros, J.-A., Flores, R., 2004. Arabidopsis thaliana has the enzymatic machinery for replicating representative viroid species of the family Pospiviroidae. Proc. Natl. Acad. Sci. USA 101, 6792–6797. https://doi.org/10.1073/pnas.0401090101.

Daròs, J.A., Elena, S.F., Flores, R., 2006. Viroids: an Ariadne's thread into the RNA labyrinth. EMBO Rep. 7, 593–598. https://doi.org/10.1038/sj.embor.7400706.

Denti, M.A., Boutla, A., Tsagris, M., Tabler, M., 2004. Short interfering RNAs specific for potato spindle tuber viroid are found in the cytoplasm but not in the nucleus. Plant J (https://doi.org/2001 [pii]).

Di Serio, F., Flores, R., Verhoeven, J.T.J., Li, S.F., Pallás, V., Randles, J.W., Sano, T., Vidalakis, G., Owens, R.A., 2014. Current status of viroid taxonomy. Arch. Virol. 159, 3467–3478. https://doi.org/10.1007/s00705-014-2200-6.

Diermann, N., Matoušek, J., Junge, M., Riesner, D., Steger, G., 2010. Characterization of plant miRNAs and small RNAs derived from potato spindle tuber viroid (PSTVd) in infected tomato. Biol. Chem. 391, 1379–1390. https://doi.org/10.1515/BC.2010.148.

Dong, Z., Han, M.-H., Fedoroff, N., 2008. The RNA-binding proteins HYL1 and SE promote accurate in vitro processing of pri-miRNA by DCL1. Proc. Natl. Acad. Sci. USA 105, 9970–9975. https://doi.org/10.1073/pnas.0803356105.

Flores, R., Di Serio, F., Navarro, B., Duran-Vila, N., Owens, R.A., 2011. Viroids and viroid diseases of plants. Stud. Viral Ecol. Microb. Bot. Host Syst. 1, 307–342. https://doi.org/10.1002/9781118025666.ch12.

Gomez, G., Martinez, G., Pallas, V., 2008. Viroid-induced symptoms in Nicotiana benthamiana plants are dependent on RDR6 activity. Plant Physiol. 148, 414–423. https://doi.org/10.1104/pp.108.120808.

Grigg, S.P., Canales, C., Hay, A., Tsiantis, M., 2005. SERRATE coordinates shoot meristem function and leaf axial patterning in Arabidopsis. Nature 437, 1022–1026. https://doi.org/10.1038/nature04052.

Horsch, R.B., Fry, J.E., Hoffmann, N.L., Eichholtz, D., Rogers, S.G., Fraley, R.T., 1985. A simple and general method for hybridization revealed the expected. Science (80-) 227, 1229–1231. https://doi.org/10.1126/science.227.4691.1229.

Itaya, A., Folimonov, A., Matsuda, Y., Nelson, R.S., Ding, B., 2001. Potato spindle tuber viroid as inducer of RNA silencing in infected tomato. Mol. Plant Microbe Interact. https://doi.org/10.1094/MPMI.2001.14.11.1332.

Itaya, A., Matsuda, Y., Gonzales, R.A., Nelson, R.S., Ding, B., 2002. Potato spindle tuber viroid strains of different pathogenicity induces and suppresses expression of common and unique genes in infected tomato. Mol. Plant Microbe Interact. 15, 990–999. https://doi.org/10.1094/MPMI.2002.15.10.990.

Itaya, A., Zhong, X., Bundschuh, R., Qi, Y., Wang, Y., Takeda, R., Harris, A.R., Molina, C., Nelson, R.S., Ding, B., 2007. A structured viroid RNA serves as a substrate for dicer-like cleavage to produce biologically active small RNAs but is resistant to RNA-induced silencing complex-mediated degradation. J. Virol. 81, 2980–2994. https://doi.org/10.1128/JVI.02339-06.

Iwata, Y., Takahashi, M., Fedoroff, N.V., Hamdan, S.M., 2013. Dissecting the interactions of SERRATE with RNA and DICER-LIKE 1 in Arabidopsis microRNA precursor processing. Nucleic Acids Res. 41, 9129–9140. https://doi.org/10.1093/nar/gkt667.

Kalantidis, K., Psaradakis, S., Tabler, M., Tsagris, M., 2002. The occurrence of CMV-specific short RNAs in transgenic tobacco expressing virus-derived double-stranded RNA is indicative of resistance to the virus. Mol. Plant Microbe Interact. 15, 826–833. https://doi.org/10.1094/MPMI.2002.15.8.826.

Katsarou, K., Mavrothalassiti, E., Dermauw, W., Van Leeuwen, T., Kalantidis, K., 2016. Combined activity of DCL2 and DCL3 is crucial in the defense against potato spindle tuber viroid. PLoS Pathog. 12, 1–24. https://doi.org/10.1371/journal.ppat.1005936.

Katsarou, K., Rao, A.L.N., Tsagris, M., Kalantidis, K., 2015. Infectious long non-coding RNAs. Biochimie 117, 37–47. https://doi.org/10.1016/j.biochi.2015.05.005.

Kofalvi, S.A., Marcos, J.F., Cañizares, M.C., Pallás, V., Candresse, T., 1997. Hop stunt viroid (HSVd) sequence variants from Prunes species: evidence for recombination between HSVd isolates. J. Gen. Virol. 78, 3177–3186. https://doi.org/10.1099/0022-1317-78-12-3177.

Kościańska, E., Kalantidis, K., Wypijewski, K., Sadowski, J., Tabler, M., 2005. Analysis of RNA silencing in agroinfiltrated leaves of Nicotiana benthamiana and Nicotiana tabacum. Plant Mol. Biol. 59, 647–661. https://doi.org/10.1007/s11103-005-0668-x.

Kotakis, C., Vrettos, N., Kotsis, D., Tsagris, M., Kotzabasis, K., Kalantidis, K., 2010. Light intensity affects RNA silencing of a transgene in Nicotiana benthamiana plants. BMC Plant Biol. 10, 220. https://doi.org/10.1186/1471-2229-10-220.

Kurihara, Y., Watanabe, Y., 2004. From the cover: arabidopsis micro-RNA biogenesis through Dicer-like 1 protein functions. Proc. Natl. Acad. Sci. USA 101, 12753–12758. https://doi.org/10.1073/pnas.0403115101.

Landry, P., Perreault, J.-P., 2005. Identification of a peach latent mosaic viroid hairpin able to act as a Dicer-like substrate. J. Virol. 79, 6540–6543. https://doi.org/10.1128/JVI.79.10.6540-6543.2005.

Landry, P., Perreault, J.P., 2004. The role of viroids in gene silencing: the model case of Peach latent mosaic viroid. Can. J. Plant Pathol. https://doi.org/10.1080/07060660409507109.

Laubinger, S., Sachsenberg, T., Zeller, G., Busch, W., Lohmann, J.U., Ratsch, G., Weigel, D., 2008. Dual roles of the nuclear cap-binding complex and SERRATE in pre-mRNA splicing and microRNA processing in Arabidopsis thaliana. Proc. Natl. Acad. Sci. USA 105, 8795–8800. https://doi.org/10.1073/pnas.0802493105.

Liu, D., Shi, L., Han, C., Yu, J., Li, D., Zhang, Y., 2012. Validation of reference genes for gene expression studies in virus-infected Nicotiana benthamiana using quantitative real-time PCR. PLoS One 7. https://doi.org/10.1371/journal.pone.0046451.

Lobbes, D., Rallapalli, G., Schmidt, D.D., Martin, C., Clarke, J., 2006. SERRATE: a new player on the plant microRNA scene. EMBO Rep. 7, 1052–1058. https://doi.org/10.1038/sj.embor.7400806.

Machida, S., Yamahata, N., Watanuki, H., Owens, R.A., Sano, T., 2007. Successive accumulation of two size classes of viroid-specific small RNA in potato spindle tuber viroid-infected tomato plants. J. Gen. Virol. https://doi.org/10.1099/vir.0.83228-0.

Markarian, N., Li, H.W., Ding, S.W., Semancik, J.S., 2004. RNA silencing as related to viroid induced symptom expression. Arch. Virol. 149, 397–406. https://doi.org/10.1007/s00705-003-0215-5.

Martín, R., Arenas, C., Daròs, J.A., Covarrubias, A., Reyes, J.L., Chua, N.H., 2007. Characterization of small RNAs derived from Citrus exocortis viroid (CEVd) in infected tomato plants. Virology 367, 135–146. https://doi.org/10.1016/j.virol.2007.05.011.

Martínez de Alba, a.E., Flores, R., Hernández, C., de Alba, A.E., Flores, R., Hernandez, C., Martinez de Alba, A.E., 2002. Two chloroplastic viroids induce the accumulation of small RNAs associated with posttranscriptional gene silencing. J. Virol. https://doi.org/10.1128/JVI.76.24.13094-13096.2002.

Masuta, C., Takanami, Y., 1989. Determination of sequence and structural requirements for pathogenicity of a cucumber mosaic virus satellite RNA (Y-satRNA). Plant Cell 1, 1165–1173. https://doi.org/10.1105/tpc.1.12.1165.

Matoušek, J., Kozlová, P., Orctová, L., Schmitz, A., Pešina, K., Bannach, O., Diermann, N., Steger, G., Riesner, D., 2007. Accumulation of viroid-specific small RNAs and increase in nucleolytic activities linked to viroid-caused pathogenesis. Biol. Chem. 388, 1–13. https://doi.org/10.1515/BC.2007.001.

Matzke, M., Kanno, T., Daxinger, L., Huettel, B., Matzke, A.J., 2009. RNA-mediated chromatin-based silencing in plants. Curr. Opin. Cell Biol. https://doi.org/10.1016/j.ceb.2009.01.025.

Mermigka, G., Verret, F., Kalantidis, K., 2016. RNA silencing movement in plants. J. Integr. Plant Biol. 58, 328–342. https://doi.org/10.1111/jipb.12423.

Minoia, S., Carbonell, A., Di Serio, F., Gisel, A., Carrington, J.C., Navarro, B., Flores, R., 2014. Specific argonautes selectively bind small RNAs derived from Potato spindle tuber viroid and attenuate viroid accumulation in vivo. J. Virol. 88, 11933–11945. https://doi.org/10.1128/JVI.01404-14.

Murashige, T., Skoog, F., 1962. A revised medium for rapid growth and bio assays with tobacco tissue cultures. Physiol. Plant 15, 473–497. https://doi.org/10.1111/j.1399-3054.1962.tb08052.x.

Navarro, B., Gisel, A., Rodio, M.E., Delgado, S., Flores, R., Di Serio, F., 2012a. Small RNAs containing the pathogenic determinant of a chloroplast- replicating viroid guide the degradation of a host mRNA as predicted by RNA silencing. Plant J. 70, 991–1003. https://doi.org/10.1111/j.1365-313X.2012.04940.x.

Navarro, B., Gisel, A., Rodio, M.E., Delgado, S., Flores, R., Di Serio, F., 2012b. Viroids: how to infect a host and cause disease without encoding proteins. Biochimie 94, 1474–1480. https://doi.org/10.1016/j.biochi.2012.02.020.

Niu, D., Lii, Y.E., Chellappan, P., Lei, L., Peralta, K., Jiang, C., Guo, J., Coaker, G., Jin, H., 2016. MiRNA863-3p sequentially targets negative immune regulator ARLPKs and positive regulator SERRATE upon bacterial infection. Nat. Commun. 7, 1–13. https://doi.org/10.1038/ncomms11324.

Owens, R.A., 2007. Potato spindle tuber viroid: the simplicity paradox resolved? Mol. Plant Pathol. 8, 549–560. https://doi.org/10.1111/j.1364-3703.2007.00418.x.

Owens, R.A., Tech, K.B., Shao, J.Y., Sano, T., Baker, C.J., 2012. Global analysis of tomato gene expression during *Potato spindle tuber viroid* infection reveals a complex array of changes affecting hormone signaling. Mol. Plant-Microbe Interact. 25, 582–598. https://doi.org/10.1094/MPMI-09-11-0258.

Palukaitis, P., 2014. What has been happening with viroids? Virus Genes 49, 175–184. https://doi.org/10.1007/s11262-014-1110-8.

Papaefthimiou, I., Hamilton, A., Denti, M., Baulcombe, D., Tsagris, M., Tabler, M., 2001. Replicating potato spindle tuber viroid RNA is accompanied by short RNA fragments that are characteristic of post-transcriptional gene silencing. Nucleic Acids Res. https://doi.org/10.1093/nar/29.11.2395.

Pfaffl, M.W., Tichopad, A., Prgomet, C., Neuvians, T.P., 2004. Determination of stable housekeeping genes, differentially regulated target genes and sample integrity: bestkeeper – excel-based tool using pair-wise correlations. Biotechnol. Lett. 26, 509–515.

Prigge, M.J., Wagner, D.R., 2001. The Arabidopsis SERRATE gene encodes a zinc-finger protein required for normal shoot development. Plant Cell 13, 1263–1280. https://doi.org/10.1105/tpc.13.6.1263.

Pumplin, N., Voinnet, O., 2013. RNA silencing suppression by plant pathogens: defence, counter-defence and counter-counter-defence. Nat. Rev. Microbiol. 11, 745–760. https://doi.org/10.1038/nrmicro3120.

Qi, Y., Pélissier, T., Itaya, A., Hunt, E., Wassenegger, M., Ding, B., 2004. Direct role of a viroid RNA motif in mediating directional RNA trafficking across a specific cellular boundary. Plant Cell Online 16, 1741–1752. https://doi.org/10.1105/tpc.021980.

Qin, C., Li, B., Fan, Y., Zhang, X., Yu, Z., Ryabov, E., Zhao, M., Wang, H., Shi, N., Zhang, P., Jackson, S., Tör, M., Cheng, Q., Liu, Y., Gallusci, P., Hong, Y., 2017. Roles of Dicer-like 2 and 4 in intra- and intercellular antiviral silencing. Plant Physiol. 174, 1067–1081. https://doi.org/10.1104/pp.17.00475.

Qu, F., Ye, X., Morris, T.J., 2008. Arabidopsis DRB4, AGO1, AGO7, and RDR6 participate in a DCL4-initiated antiviral RNA silencing pathway negatively regulated by DCL1. Proc. Natl. Acad. Sci. USA 105, 14732–14737. https://doi.org/10.1073/pnas.0805760105.

Raczynska, K.D., Stepien, A., Kierzkowski, D., Kalak, M., Bajczyk, M., McNicol, J., Simpson, C.G., Szweykowska-Kulinska, Z., Brown, J.W.S., Jarmolowski, A., 2014. The SERRATE protein is involved in alternative splicing in Arabidopsis thaliana. Nucleic Acids Res. 42, 1224–1244. https://doi.org/10.1093/nar/gkt894.

Rao, A.L.N., Kalantidis, K., 2015. Virus-associated small satellite RNAs and viroids display similarities in their replication strategies. Virology 479–480, 627–636. https://doi.org/10.1016/j.virol.2015.02.018.

Ruiz-Ferrer, V., Voinnet, O., 2009. Roles of plant small RNAs in biotic stress responses. Annu. Rev. Plant Biol. 60, 485–510. https://doi.org/10.1146/annurev.arplant.043008.092111.

Schauer, S.E., Jacobsen, S.E., Meinke, D.W., Ray, A., 2002. *DICER-LIKE1*: blind men and elephants *Arabidopsis* development. Trends Plant Sci. 7, 487–491.

Schwind, N., Zwiebel, M., Itaya, A., Ding, B., Wang, M.B., Krczal, G., Wassenegger, M., 2009. RNAi-mediated resistance to Potato spindle tuber viroid in transgenic tomato expressing a viroid hairpin RNA construct. Mol. Plant Pathol. 10, 459–469. https://doi.org/10.1111/j.1364-3703.2009.00546.x.

Shimura, H., Pantaleo, V., Ishihara, T., Myojo, N., Inaba, J. ichi, Sueda, K., Burgyán, J., Masuta, C., 2011. A viral satellite RNA induces yellow symptoms on tobacco by targeting a gene involved in chlorophyll biosynthesis using the RNA silencing machinery. PLoS Pathog. 7, 1–12. https://doi.org/10.1371/journal.ppat.1002021.

Smith, N.A., Eamens, A.L., Wang, M.B., 2011. Viral small interfering RNAs target host genes to mediate disease symptoms in plants. PLoS Pathog. 7, 1–9. https://doi.org/10.1371/journal.ppat.1002022.

Speth, et al., 2018. Arabidopsis RNA processing factor SERRATE regulates the transcription of intronless genes. Unpublished. pp. 45220–45220. ‹https://doi.org/10.1111/ijlh.12426›.

Tabler, M., Sänger, H.L., 1984. Cloned single- and double-stranded DNA copies of potato spindle tuber viroid (PSTV) RNA and co-inoculated subgenomic DNA fragments are infectious. EMBO J. 3, 3055–3062.

Tabler, M., Tsagris, M., 2004. Viroids: petite RNA pathogens with distinguished talents. Trends Plant Sci. https://doi.org/10.1016/j.tplants.2004.05.007.

Tabler, M., Tzortzakaki, S., Tsagris, M., 1992. Processing of linear longer-than-unit-length potato spindle tuber viroid RNAs into infectious monomeric circular molecules by a G-specific endoribonuclease. Virology 190, 746–753. https://doi.org/10.1016/0042-6822(92)90912-9.

Torchetti, E.M., Pegoraro, M., Navarro, B., Catoni, M., Di Serio, F., Noris, E., 2016. A nuclear-replicating viroid antagonizes infectivity and accumulation of a geminivirus by upregulating methylation-related genes and inducing hypermethylation of viral DNA. Sci. Rep. 6, 1–11. https://doi.org/10.1038/srep35101.

Tsagris, E.M., de Alba, Á.E.M., Gozmanova, M., Kalantidis, K., 2008. Viroids. Cell. Microbiol. https://doi.org/10.1111/j.1462-5822.2008.01231.x.

Varkonyi-gasic, E., Wu, R., Wood, M., Walton, E.F., Hellens, R.P., 2007. Protocol: a highly sensitive RT-PCR method for detection and quantification of microRNAs. Plant Methods 3, 1–12. https://doi.org/10.1186/1746-4811-3-12.

Voisin, D., Nawrath, C., Kurdyukov, S., Franke, R.B., Reina-Pinto, J.J., Efremova, N., Will, I., Schreiber, L., Yephremov, A., 2009. Dissection of the complex phenotype in cuticular mutants of Arabidopsis reveals a role of SERRATE as a mediator. PLoS Genet. 5. https://doi.org/10.1371/journal.pgen.1000703.

Wang, M.-B., Bian, X.-Y., Wu, L.-M., Liu, L.-X., Smith, N.A., Isenegger, D., Wu, R.-M., Masuta, C., Vance, V.B., Watson, J.M., Rezaian, A., Dennis, E.S., Waterhouse, P.M., 2004. On the role of RNA silencing in the pathogenicity and evolution of viroids and viral satellites. Proc. Natl. Acad. Sci. USA 101, 3275–3280. https://doi.org/10.1073/pnas.0400104101.

Wang, Y., Shibuya, M., Taneda, A., Kurauchi, T., Senda, M., Owens, R.A., Sano, T., 2011. Accumulation of Potato spindle tuber viroid-specific small RNAs is accompanied by specific changes in gene expression in two tomato cultivars. Virology 413, 72–83. https://doi.org/10.1016/j.virol.2011.01.021.

Wang, Z., Ma, Z., Castillo-González, C., Sun, D., Li, Y., Yu, B., Zhao, B., Li, P., Zhang, X., 2018. SWI2/SNF2 ATPase CHR2 remodels pri-miRNAs via Serrate to impede miRNA production. Nature 557, 516–521. https://doi.org/10.1038/s41586-018-0135-x.

Xie, M., Zhang, S., Yu, B., 2015. microRNA biogenesis, degradation and activity in plants. Cell. Mol. Life Sci. https://doi.org/10.1007/s00018-014-1728-7.

Yang, L., Liu, Z., Lu, F., Dong, A., Huang, H., 2006. SERRATE is a novel nuclear regulator in primary microRNA processing in Arabidopsis. Plant J. 47, 841–850. https://doi.org/10.1111/j.1365-313X.2006.02835.x.

Zheng, Y., Wang, Y., Ding, B., Fei, Z., 2017. Comprehensive transcriptome analyses reveal that potato spindle tuber viroid triggers genome-wide changes in alternative splicing, inducible trans-acting activity of phasiRNAs and immune responses (00247-17). J. Virol. JVI. https://doi.org/10.1128/JVI.00247-17.